

RESEARCH ARTICLE

Proteomic profile of mouse fibroblasts with a targeted disruption of the peroxisome proliferator activated receptor- β/δ gene

Jürgen Adamkiewicz, Kerstin Kaddatz, Markus Rieck, Bernhard Wilke, Sabine Müller-Brüsselbach and Rolf Müller

Institute of Molecular Biology and Tumor Research (IMT), Philipps University, Marburg, Germany

The peroxisome proliferator activated receptor- β (PPAR β) plays an essential role in lipid metabolism, immune modulation, differentiation and cell proliferation. There is also strong evidence for a function in oncogenesis and tumor vascularization, but the underlying molecular mechanisms remain elusive. In the present study, we have used fibroblasts derived from *Pparb* wild-type and null mice to determine by 2-DE and PMF analysis the contribution of PPAR β to the protein profile of fibroblasts. Thirty-one differentially expressed proteins of different functional categories were identified. For at least two proteins a role in tumorigenesis and/or tumor vascularization has previously been reported: while the calcium intracellular channel-4 (CLIC4) was expressed at lower levels in *Pparb* null cells, expression of the cellular retinol binding protein 1 (CRBP1) was enhanced. *Clic4* and *Crbp1* gene expression patterns observed in different experimental settings *in vitro* and *in vivo* confirmed the proteomics data. Our findings indicate that the expression of a defined set of proteins is altered in fibroblasts and endothelial cells from *Pparb* null mice, that this is due to aberrant gene regulation, and that the altered expression of these proteins is consistent with the tumor vascularization phenotype of *Pparb* null mice.

Received: December 12, 2006

Revised: January 9, 2007

Accepted: January 22, 2007

Keywords:

Calcium intracellular channel-4 (CLIC4) / Cellular retinol binding protein 1 (CRBP1) / Endothelial cells / Fibroblasts / PPAR β

1 Introduction

The peroxisome proliferator activated receptor- β (PPAR β), also known as PPAR δ , is a nuclear receptor with essential functions in diverse biochemical and biological processes, including lipid metabolism, wound healing and immune

modulation, and is a potential new drug target for the treatment of major human diseases such as obesity, metabolic syndrome, inflammation and atherosclerosis [1, 2]. PPAR β also promotes differentiation and inhibits proliferation in different cell types [3–8]. There is also clear, although partially conflicting, evidence for a role of PPAR β in tumorigenesis [9]. Loss of tumorigenicity has been reported for the human colon carcinoma cells after *Pparb* deletion [10], and the growth of intestinal polyps in *APC^{Min}* mice is potentiated by treatment with a synthetic PPAR β agonist GW501516 [11]. In a more recent study, however, polyp formation induced by the chemical carcinogen azoxymethane was attenuated by a PPAR β agonist [12]. In agreement with the latter observation, the genetic disruption of *Pparb* enhanced intestinal polyp growth in both *APC^{Min}* and azoxymethane-treated mice [13, 14], even though in one study this effect was visible only in larger tumors [15]. These apparent dis-

Correspondence: Rolf Müller, Institute of Molecular Biology and Tumor Research (IMT), Philipps University, Emil-Mannkopff-Strasse 2, 35032 Marburg, Germany

E-mail: rmueller@imt.uni-marburg.de

Fax: +49-6421-2868923

Abbreviations: CLIC1/4, calcium intracellular channel-1/-4; CRBP1, cellular retinol binding protein 1; EC, endothelial cell; HUVEC, human umbilical vein endothelial cell; PPAR β , peroxisome proliferator activated receptor-beta;

crepancies may be due the fact that these studies did not distinguish between a role for PPAR β in the tumor cells and the recruited host cells with potentially opposing effects on tumor growth. This issue is of particular relevance in view of recent findings pointing to a role for PPAR β in angiogenic endothelial cells. Thus, the PPAR β agonist L-165041 has been reported to promote endothelial cell survival, which correlated with a PPAR β -dependent up-regulation of the anti-apoptotic 14-3-3 α gene [16]. In another study, the PPAR β agonist GW501516 was shown to enhance endothelial morphogenesis both *in vitro* and *in vivo* concomitant with the induction of vascular endothelial growth factor expression [17]. Finally, our own work (Müller-Brüsselbach *et al.*, manuscript in preparation) revealed a severe defect in tumor vascularization in *Pparb* null mice [18]. This phenotype apparently arises from the hyperproliferation of ECs and inhibition of microvessel maturation specifically in the tumor microenvironment, thus leading to endothelial hyperplasia and microvessel dysfunction. The role of PPAR β in stromal cell types, such as fibroblasts and endothelial cells, is therefore of particular interest.

To date, the role of PPAR β in determining the transcriptome or proteome of cell types characteristic of the tumor stroma, such as fibroblasts or endothelial cells (ECs), has not been systematically addressed. In the present study, we have made use of mice with targeted disruptions of both *Pparb* alleles to establish fibroblasts lacking PPAR β protein. These *Pparb* null cells were compared by 2-DE and MALDI-TOF analysis to *Pparb* wild-type cells established in the identical way. As expected, several of the differentially expressed proteins represent components of intermediary metabolism, but at least two other proteins deserve particular attention with respect to a regulatory role in tumorigenesis and/or tumor vascularization. These are the ~~calcium~~ intracellular channel-4 (CLIC4) [19, 20] and the cellular retinol binding protein 1 (CRBP1). Both CLIC4 and CRBP1 have previously been associated with tumorigenesis [21–32]. CLIC4 has also been associated with angiogenesis [33] and myofibroblast differentiation [34], essential processes associated with the tumor stroma. For both genes, we were also able to demonstrate aberrant regulation at the level of transcription in fibroblasts and ECs from *Pparb* null mice. *Clic4* and *Crbp1* are therefore novel candidate genes whose dysregulation may contribute to the tumor vascularization phenotype of *Pparb* null mice.

2 Materials and methods

2.1 Reagents

Ammonium persulfate, CHAPS, DTT, iodoacetamide (IAA), SDS, TEMED, thiourea, urea, Immobilin DryStrip (IPG-strip, 24 cm, pH range 3–11 nonlinear), and IPG buffer were from Amersham Biosciences (Freiburg, Germany). Acrylamide/bis (30%) solution (37.5:1), agarose for IEF, and Tris

were purchased from Roth (Karlsruhe, Germany). Glycerol, TFA, and bromophenol blue were from Serva (Heidelberg, Germany), 2-hydroxyethyl disulfide (HED), protease inhibitors and silver nitrate from Sigma-Aldrich (Taufkirchen, Germany). Protein molecular weight marker for SDS-PAGE analysis was from Fermentas (St. Leon-Rot, Germany), the Quick Start Bradford Protein Assay from BioRad (Munich, Germany), and the Qproteome Cell Compartment Kit from Qiagen (Hilden, Germany). Acetone, ACN, ethanol, and water for MS were HPLC grade and purchased from Merck (Schwalbach, Germany). Porcine trypsin for PMF analysis was from Promega (Mannheim, Germany), CHCA and peptide calibration standard were purchased from Bruker (Bremen, Germany).

2.2 Fibroblasts from *Pparb* wild-type and null mice

Pparb wild-type and null mouse strains have previously been described [18]. All experiments were performed with mice backcrossed six generations with the C57BL/6N strain. Primary cultures of mouse lung fibroblasts were established from fetal lungs removed aseptically from day 18–19 embryos. Lungs were cut into small pieces and incubated for 30 min at 37°C in cell culture grade trypsin solution. Following centrifugation, cells and remaining tissue pieces were cultured in DMEM supplemented with antibiotics, fungicide, and 20% FCS. Cell lines were established after ~15 passages and grown in DMEM plus 10% FCS.

2.3 Endothelial cell cultures

Thoracic aortas were surgically removed from 2–3-month-old mice and associated periaortic tissue was carefully removed. Aortic rings of about 1-mm length were cut, placed on matrigel and cultured for 2–4 weeks in EGM-2 medium (Cambrex, Copenhagen, Denmark). Outgrowing capillary forming cells were isolated from matrigel by collagenase digestion followed by cultivation on collagen-coated cell culture plates in endothelial cell growth medium. Cell lines were established after ~15 passages. The endothelial nature of these cells was verified by immunostaining and PCR analysis, which showed strong expression of the endothelial markers Flt-1, CD105/endoglin and aquaporin-1, and a lack of the monocyte/macrophage markers CD68 and F4/80 (data not shown). Human umbilical vein endothelial cells (HUVECs) were prepared as described [35] and cultured in EGM-2 medium for maximum 5 passages.

2.4 Matrigel plugs

Matrigel plugs were established using the BD Matrigel Matrix (Becton Dickinson) as described by the manufacturer. In brief, 500 μ L liquefied matrigel containing 100 nM PGE₂ and 0.6 μ g/mL FGF-2 were injected subcutaneously and plugs were removed 3 days later for analysis.

2.5 Sample preparation for 2-DE

Cells at ~80% confluence were washed with 20 mL of ice cold PBS and immediately lysed in 2-D lysis buffer (8 M urea, 2 M thiourea, 4% CHAPS, 0.1 M HED) containing a protease inhibitor cocktail. Alternatively, cells were fractionated into cytosol, membrane and nuclear fractions using the Qiagen Qproteome Cell Compartment Kit as described by the manufacturer. In some experiments (see Table 1 for details), we also prepared fractions enriched in mitochondria. All samples in 2-D lysis buffer were centrifuged at $100\,000 \times g$ for 30 min to remove insoluble debris prior to 2-DE. Protein concentrations were determined using the Quick Start Bradford Protein Assay (BioRad). Samples were prepared in at least two independent experiments.

2.6 2-DE

2-DE was performed as initially described by O'Farrell [36] and Klose [37]. First-dimension IEF was performed using the Amersham Biosciences Ettan IPGphor; second-dimension SDS-PAGE was carried out using the Ettan DALT Six System. Samples in 2-D lysis buffer containing up to 2 mg protein were supplemented with IPG buffer and bromophenol blue (final concentrations 0.5% and 0.001%, respectively), and applied to 24-cm IPG strips by in-gel rehydration in a final volume of 550 μ L according to the manufacturer's instructions. Proteins were focused for up to 110 000 Vh at a maximum voltage of 8000 V. Following IEF, proteins were reduced and alkylated by successively soaking the IPG strips in equilibration solution (6 M urea, 2% SDS, 30% glycerol, 50 mM Tris-HCl, pH 8.8, 0.001% bromophenol blue) containing 30 mg/mL DTT and 50 mg/mL IAA for 15 min at room temperature. The equilibrated IPG strips were sealed with 0.5% agarose on top of the SDS-PAGE gels (21 cm \times 25 cm; 12.5% or 8–15% gradient polyacrylamide gels). SDS-PAGE was carried out using the Tris-glycine-SDS buffer system (25 mM Tris, 192 mM glycine, and 0.1% SDS) at 2.5 W/gel for 30 min followed by 1 W/gel until the dye front reached the bottom edge of the gel. Protein spots were visualized by staining with an MS-compatible silver stain [38].

2.7 Image analysis

2-DE protein patterns were digitalized using a high-resolution scanner (LinScan 1450, Heidelberg, Germany). Spot detection, quantitation, and analysis were performed using the ImageMaster 2D Platinum Software, Version 5.0 (Amersham Biosciences). In some cases intensity normalization using scatter plots was applied to correct for differences in sample loading or staining intensities. Pairs of gels with protein samples from *Pparb* wild-type and null cells run under identical conditions were analyzed for differentially stained proteins.

2.8 Protein identification

Protein spots of interest were excised, washed and processed for in-gel trypsin digest. In short, gel pieces of about 2-mm diameter were successively washed in (i) 0.1% TFA, (ii) 0.1% TFA in 60% ACN, (iii) 0.1% TFA in 100% ACN, and (iv) 100% ACN. Following air drying for 60 min, the gel pieces were rehydrated in 20 mM ammonium hydrogen carbonate containing 15 μ g/mL porcine trypsin and digested at 40°C overnight. Peptides were eluted with 0.1% TFA and applied to CHCA thin layers on AnchorChip targets according to the manufacturers' instructions (Bruker). PMF analysis was performed using an Autoflex MALDI-TOF mass spectrometer (Bruker), peak lists were sent to MASCOT PMF search (<http://www.matrixscience.com>) using the Swiss-Prot protein database. All MASCOT search results were critically evaluated with respect to the observed molecular weight and *pI* values of the protein analyzed.

2.9 Immunoblotting

Cells at near confluence were washed with 20 mL ice-cold PBS and lysed in SDS sample buffer (125 mM Tris, 4% SDS, 20% glycerol, 5% β -mercaptoethanol, and traces of bromophenol blue). Protein concentrations were determined using the 2-D Quant kit (Amersham), and equal amounts of protein were separated on duplicate 12% gels by SDS-PAGE. Proteins were transferred to Immobilon-P (Millipore, Schwalbach, Germany), and membranes were blocked with 3% BSA in PBS for 60 min at room temperature. Incubation with primary and peroxidase-labeled secondary antibody was carried out for 1 h each, followed by three washing steps with 0.05% Tween-20 in PBS, respectively. Antibody binding was revealed by chemiluminescence. The polyclonal rabbit antibody against CLIC4 was raised against the N-terminal peptide SMPLNGLKEEDKEPL. This peptide is absent from all other mouse and human proteins represented in the Swiss-Prot database, including the other CLIC family members. The specificity of the antibody was further verified by the absence of detectable immunoreactivity in cells with low *Clic4* expression (data not shown). The mouse-anti-CRBP1 mAb (ab24090) was purchased from Abcam plc (Cambridge, UK). Peroxidase-labeled goat anti-rabbit IgG was from Cell Signaling/New England Biolabs (Frankfurt, Germany).

2.10 Quantitative PCR (qPCR)

RNA was isolated using the Nucleospin RNA II kit (Macherey-Nagel, Düren, Germany). cDNA was synthesized from 1 μ g RNA using oligo(dT) primers and the Omniscript kit (Qiagen). qPCR was performed in a Mx3000P Real-Time PCR system (Stratagene, La Jolla, CA, USA) for 40 cycles at an annealing temperature of 57–58°C. PCR reactions were carried out using the Absolute QPCR SYBR Green Mix (Abgene, Hamburg, Germany) and a primer concentration of 0.2 μ M following the manufacturer's instructions. Mouse

Table 1. Differentially expressed proteins in *Pparb* wild-type and null fibroblasts

Entry name	Accession no.	Name	Level in <i>Pparb</i> ^{-/-}	Subcell. fraction ^{a)}	No. of expts. ^{b)}	Mol. mass [kDa] ^{c)}	pI ^{d)}	MASCOT score	Peptides identified ^{e)}	Sequence coverage ^{f)}
Putative regulatory proteins										
CLIC1_mouse	Q9Z1Q5	Chloride intracellular channel protein 1	Down	C, M	4	26.9	5.1	150	18	59.2
CLIC4_mouse	Q9QYB1	Chloride intracellular channel protein 4	Down	W, C	3	28.6	5.5	221	19	79.0
DDAH2_mouse	Q99LD8	<i>N</i> ⁶ , <i>N</i> ⁶ -dimethylarginine dimethylaminohydrolase 2	Up	Mt	2	29.6	5.7	123	15	59.6
GBLP_mouse	P68040	Guanine nucleotide-binding protein beta subunit 2-like 1	Up	W, C	3	35.0	7.6	343	25	87.4
PA2G4_mouse	P50580	Proliferation-associated protein 2G4	Up	W, N	5	43.6	6.4	161	37	73.1
PRDX1_mouse	P35700	Peroxiredoxin 1	Up	C	2	22.2	8.3	108	7	30.7
RET1_mouse	Q00915	Retinol-binding protein I, cellular	Up	C	5	15.7	5.1	236	23	85.8
STRAP_mouse	Q9Z1Z2	Serine-threonine kinase receptor-associated protein	Up	C	4	38.5	5.0	185	20	60.1
TXNL1_mouse	Q8CDN6	Thioredoxin-like protein 1	Up	C	3	32.1	4.8	150	13	56.4
S10A6_mouse	P14069	Calcyclin	Down	C	2	10.1	5.3	65	8	46.1
SEP11_mouse	Q8C1B7	Septin-11	Up	Mt	2	49.6	6.3	219	27	38.1
PCBP1_mouse	P60335	Poly(rC)-binding protein 1	Up	W	3	37.5	6.7	110	17	52.8
Metabolic pathways										
AATM_mouse	P05202	Aspartate aminotransferase, mitochondrial	Up	M, C, Mt	3	44.6	9.0	156	22	42.6
AK1A1_mouse	Q9J1I6	Alcohol dehydrogenase (NADP+)	Up	C	2	36.5	6.9	289	23	66.0
ALDOA_mouse	P05064	Fructose-bisphosphate aldolase A	Down	C, N	3	39.2	8.4	127	14	44.6
ENOA_mouse	P17182	Alpha enolase	Up	W, C	3	47.0	6.4	196	25	67.2
GALK1_mouse	Q9R0N0	Galactokinase	Up	W, C	3	42.2	5.2	85	11	42.2
KCRB_mouse	Q04447	Creatine kinase, B chain	Down	C	2	42.7	5.4	146	21	58.5
PRPS1_mouse	Q9D7G0	Ribose-phosphate pyrophosphokinase I	Up	Mt	2	34.7	6.6	130	13	42.0
LDHB_mouse	P16125	L-Lactate dehydrogenase B chain	Up	W, C	4	36.4	5.7	222	24	70.9
Protein synthesis and transport										
EF2_mouse	P58252	Elongation factor 2	Up	W, C	3	95.2	6.4	97	27	29.9
GRP75_mouse	P38647	Stress-70 protein, splice isoform 2, mitochondrial precursor	Up	N	3	68.6	5.5	196	25	41.4
HSPB1_mouse	P14602	Heat-shock protein beta-1	Down	C	5	23.0	6.1	168	13	74.6
M6PBP_mouse	Q9DBG5	Mannose-6-phosphate receptor binding protein 1	Up	C	2	47.3	5.5	153	18	54.2
P4H1_mouse	Q60715	Prolyl 4-hydroxylase alpha-1 subunit (precursor)	Down	N	2	59.0	5.6	298	33	57.3
PPCE_mouse	Q9QUR6	Prolyl endopeptidase	Down	C	2	80.8	5.4	359	32	64.4
PPID_mouse	Q9CR16	40 kDa peptidyl-prolyl <i>cis-trans</i> isomerase	Up	C	3	41.0	7.1	138	11	34.7
Structural organization										
CLCA_mouse	O08585	Clathrin light chain A	Up	C, N	2	25.6	4.5	77	7	21.7
CRYAB_mouse	P23927	Alpha crystallin B chain	Down	C, N	6	20.1	6.8	105	10	57.1
FSC1_mouse	Q61553	Fascin	Up	Mt	3	54.3	6.2	173	24	52.8
TAGL_mouse	P37804	Transgelin	Down	N	2	22.4	8.9	115	18	63.5

a) C, cytosol fraction, M, membrane fraction, Mt, mitochondrial fraction, N, nuclear fraction, W, whole cell extract.

b) Number of individual experiments performed with different cell extracts or fractions.

c) Calculated molecular mass (Swiss-Prot).

d) Theoretical pI based on the primary structure of the protein (Swiss-Prot).

e) Total number of matched peaks identified by MASCOT PMF search after MALDI-TOF analysis.

f) Sequence coverage of the protein in percentage obtained by MASCOT PMF identifications.

L27 and human Gapdh were used as normalizer. Pooled RNA from mouse aorta cells or from mouse fibroblasts served as the calibrator, as indicated in the respective figure

legends. Comparative expression analyses were statistically analyzed by Student's *t*-test (two-tailed, equal variance). The following primers were used in the present study:

muPparb_forw: 5'-CTCCATCGTCAACAAAGACG; muPparb_rev: 5'-TCTTCTTTAGCCACTGCATC; muClic4_forw: 5'-AGCTTTCACCAAAGCACCCAGAGT; muClic4_rev: 5'-TGT CATCTCATCGCCGTCCAGAAA; muCrbp1_forw: 5'-CTGAG-CAATGAGAATTTCGAGGA; muCrbp1_rev: 5'-GCGGTCCG-TCTATGCCTGTC; Arp0_for: 5'-AGATGCAGCAGATCCGC-AT; Arp0_rev: 5'-GTGGTGATACCTAAAGCCTG; muL27_forw: 5'-AAAGCCGTCATCGTGAAGAAC; muL27_rev: 5'-GCTGT-CACTTTCCGGGGATAG; huClic4_forw: 5'-TGAA-AGCATAG-GAAACTGCC; huClic4_rev: 5'-ACATCCGTT-TTGAC-TTCACTGT; huGapdh_forw: 5'-CGT CTT CAC CAC CAT GGA GA; huGapdh_rev: 5'-CGG CCA TCA CGC CAC AGT TT

3 Results and discussion

3.1 Expression profiling of *Pparb* wild-type and null fibroblasts

Fetal lung fibroblasts were established from both *Pparb* wild-type and null mice. Two lines of each genotype were used to determine their protein profile by 2-DE. Whole cell extracts

as well as fractions enriched for cytoplasmic, membrane, mitochondrial, nuclear, and cytoskeletal proteins were used for this study. Using broad range IPG strips, up to 1400 different spots were detectable in a gel depending on the type of fractionation. Figure 1 shows an example 2-DE of the cytosol fraction from wild-type fibroblasts. In total, approximately 2000 protein spots were identified in different subcellular fractions. The intensities of these spots were compared between *Pparb* wild-type and null cells in a total of 30 experiments. Differentially stained proteins were carefully selected taking into account the limited dynamic range of the silver staining and the possibility of locally inhomogeneous resolution or staining of proteins. Only proteins showing clearly differential staining next to neighboring protein spots of equal intensities (exemplified in Fig. 2 below) were chosen for PMF analysis. Table 1 gives a detailed summary of the proteins that were differentially stained in at least two individual experiments. These 31 proteins were grouped in four functional categories: (i) putative regulatory proteins, (ii) metabolic pathways, (iii) protein synthesis and transport, and (iv) structural organization (Fig. 3). Out of these, the first category is of particular interest since these proteins include potential components of intracellular signaling networks

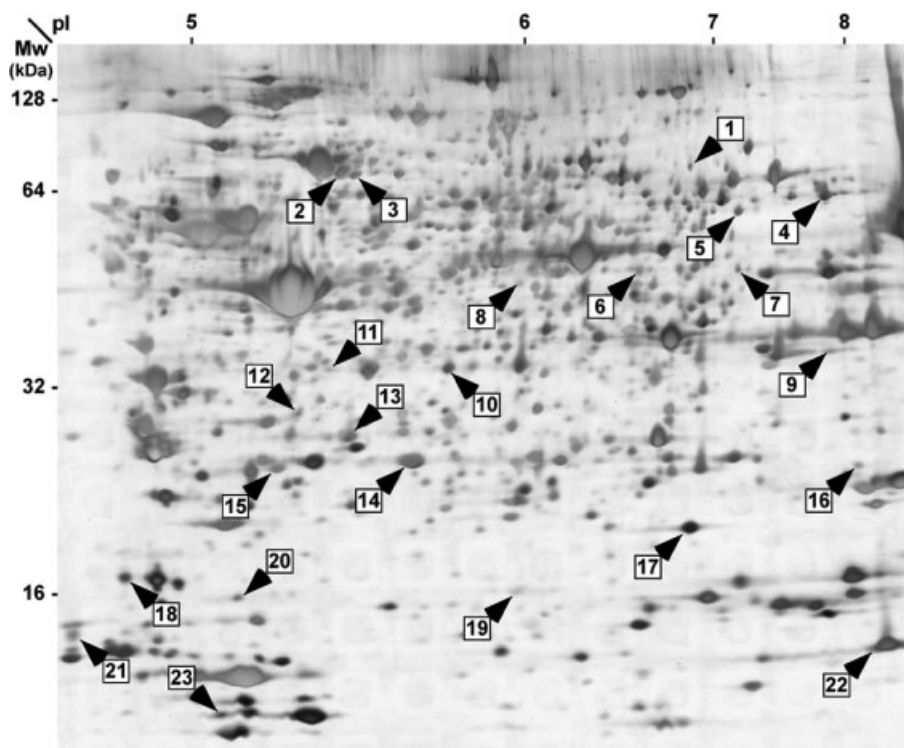


Figure 1. 2-D map of the cytosolic fraction from *Pparb* wild-type fibroblasts (silver-stained gel). Examples of proteins identified by MALDI-TOF are indicated by arrows and annotated with Swiss-Prot accession nos. and entry names. 1: Q9EQF6 (DPYL5_MOUSE); 2: P14824 (ANXA6_MOUSE); 3: Q99K51 (PLST_MOUSE); 4: P06745 (G6PI_MOUSE); 5: Q91ZJ5 (UGPA2_MOUSE); 6: O88844 (IDHC_MOUSE); 7: Q922H4 (Q922H4_MOUSE); 8: Q6PFG7 (Q6PFG7_MOUSE); 9: P06151 (LDHA_MOUSE); 10: O35640 (ANXA8_MOUSE); 11: O35887 (CALU_MOUSE); 12: Q9Z1Q5 (CLIC1_MOUSE); 13: Q9QYB1 (CLIC4_MOUSE); 14: P14602 (HSPB1_MOUSE); 15: Q9R0P9 (UCHL1_MOUSE); 16: O09061 (PSB1_MOUSE); 17: P23927 (CRYAB_MOUSE); 18: Q9WTX5 (SKP1_MOUSE); 19: P08228 (SODC_MOUSE); 20: Q9CQI3 (GMFB_MOUSE); 21: P62204 (CALM_MOUSE); 22: P62962 (PROF1_MOUSE); 23: P50543 (S10AB_MOUSE).

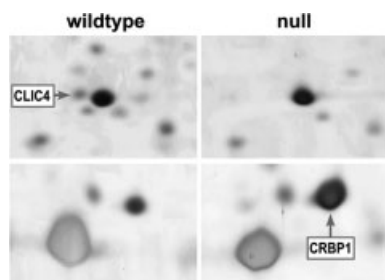


Figure 2. Sections of 2-D gels showing reduced levels of CLIC4 (top) and an increase in CRBP1 protein (bottom) in *Pparb* null compared to wild-type fibroblasts.

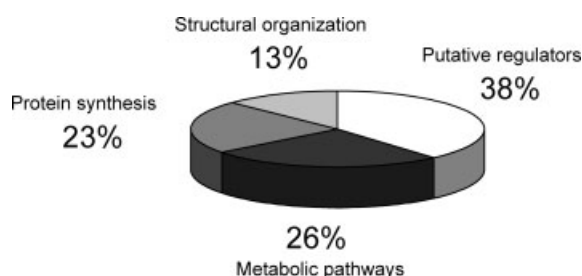


Figure 3. Functional classification of proteins differentially expressed in *Pparb* wild-type and null mouse fibroblasts based on the data in Table 1.

participating in the regulation of cell proliferation, differentiation, survival and angiogenesis. On the other hand, the identification of eight proteins figuring in metabolic pathways is consistent with PPAR β 's role in intermediary metabolism, thus confirming the experimental approach.

3.2 Chloride intracellular channel proteins

Our proteomic analysis identified two members of the chloride intracellular channel protein family, CLIC1 and CLIC4, as proteins that are expressed at higher levels in *Pparb* wild-type versus null cells (Table 1; Fig. 2, top). The CLICs have recently gained much attention due to their participation in various cellular processes, including cell proliferation [19–21, 24, 33, 34, 39]. CLIC4 in particular seems to be closely associated with tumorigenesis [22], since its expression is regulated by p53 [21], Myc [24] and transforming growth factor- β [34]. Furthermore, CLIC4 has been reported to suppress apoptosis [22] and to play an essential role in angiogenesis by orchestrating endothelial proliferation and differentiation [33]. Consistent with these observations, CLIC4 expression is modulated during pathological angiogenesis in tumor microvessels [33]. Furthermore, CLIC4 figures in the differentiation of myofibroblasts [34], another important cell type of the tumor stroma. We therefore sought to confirm the differential expression of CLIC4 in *Pparb* wild-type and null cells by an independent method. Since antibodies recogniz-

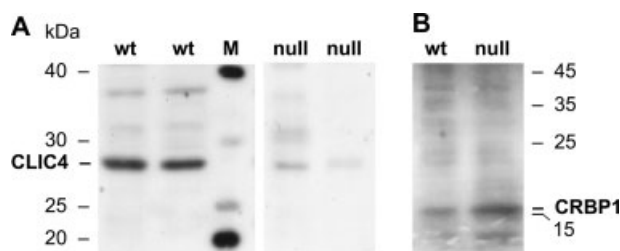


Figure 4. Immunoblot analysis of CLIC4 (A) and CRBP1 (B) in normally growing *Pparb* wild-type and null mouse fibroblasts. (A) Two independent fibroblast lines of each genotype are shown.

ing specific CLIC proteins were not available to us, we generated a polyclonal rabbit antiserum against a N-terminal peptide common to mouse, rat and human CLIC4 (see Section 2.9 for details). Using this antiserum we were able to confirm decreased expression of CLIC4 in *Pparb* null fibroblasts (Fig. 4A). CLIC4 has previously been associated with microvascular maturation [33], suggesting that its decreased expression in *Pparb* null mice may contribute to the perturbation of tumor vascularization observed in these mice (see Section 1).

3.3 CRBP1

CRBP1 showed an opposite pattern of expression, *i.e.* a higher level in *Pparb* null cells (Table 1; Fig. 2, bottom). Increased expression of CRBP1 in *Pparb* null fibroblasts was also confirmed by immunoblotting (Fig. 4B). CRBP1 is involved in vitamin A metabolism and intracellular transport of retinoids, thus influencing the activity of the nuclear retinoic acid receptors RAR and RXR [40]. Down-regulation of CRBP1 occurs in various human cancers [25–29, 31, 32, 41], and has recently been shown to affect the PI3K/Akt survival pathway [42]. Of note, the RAR and RXR agonists all-*trans* retinoic acid (ATRA) and 9-*cis* retinoic acid (9-*cis* RA), respectively, regulate target genes involved in cancer cell proliferation, differentiation and capillary formation [30], thus providing another link to the tumor vascularization phenotype in *Pparb* null mice.

3.4 PPAR β -regulated expression of the *Clc4* and *Crbp1* genes

We next asked whether transcriptional regulation contributes to the observed genotype-related differences in CLIC4 and CRBP1 expression. We therefore compared the levels of *Clc4* and *Crbp1* mRNA in two independent fibroblast lines of each genetic background (*Pparb* wild-type and null). The data in Fig. 5 fully confirm the observed pattern of protein expression: *Clc4* mRNA levels were 4- to 8-fold higher in wild-type cells, whereas *Crbp1* expression was 3- to 10-fold higher in *Pparb* null fibroblasts. Reduced *Clc4* expression was also seen in *Pparb* null aortic ECs (Fig. 6). In

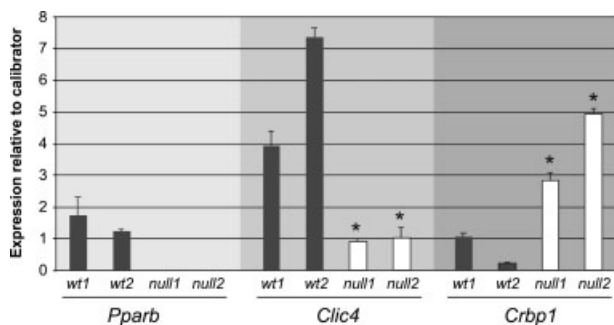


Figure 5. Differential expression of *Pparb* (control), *Clic4* and *Crbp1* genes in *Pparb* wild-type (black bars) and null mouse fibroblasts (white bars). mRNAs were extracted and analyzed by qPCR. *L27* was used as the normalizer, and pooled mouse fibroblast RNA served as the calibrator. Calibrator Ct values for *Clic4*, *CRBP1* and *L27* were 21.5, 22.4 and 18.5, respectively. Data represent average values of triplicate samples, error bars show SD. *Significant difference between *Pparb* wild-type and null mouse fibroblasts ($p < 0.05$; Student's *t*-test, two-tailed, equal variance).

addition, *Clic4* was inducible by the agonist GW501516 in wild-type ECs (49% increase), but not in the corresponding *Pparb* null aorta cells (Fig. 6). We also analyzed *Clic4* expression in HUVECs at different times after GW501516 stimulation, which confirmed our results with mouse aorta ECs. *Clic4* RNA levels remained slightly below the expression in non-stimulated cells for 8 h, and increased by 89–134% at 18–24 h after GW501516 stimulation (Fig. 6b). This type of kinetics suggests that *Clic4* is not a direct target gene of PPAR β but is rather regulated by a PPAR β initiated signaling cascade.

While *Clic4* has previously not been associated with PPAR-mediated regulation, *Crbp1* has been reported to be positively regulated by PPAR β and a PPAR β agonist in hepatic stellate cells [43]. This is in obvious contrast to the increased expression of *Crbp1* in *Pparb* null ECs and fibroblasts observed in the present study. PPAR β has been reported to regulate transcription by different mechanisms, which include the interaction of DNA-bound PPAR β with multiple coactivators, corepressors and the retinoic acid receptor RxR [44–46], as well as the DNA-independent binding of the transcriptional repressor BCL6 [47]. Therefore, the availability and concentration of specific transcription factors as well as their stoichiometry will ultimately determine the effect on a given target gene. It is likely that the discrepancies eluded to above are a reflection of these complex and largely unknown regulatory mechanisms that probably include cell type-specific components.

Finally, we investigated whether *Clic4* and *Crbp1* expression would also show *Pparb*-dependent differences in an *in vivo* model of tumor angiogenesis. Matrigel matrix was mixed with pro-angiogenic growth factors and injected subcutaneously into both *Pparb* wild-type and null mice, where

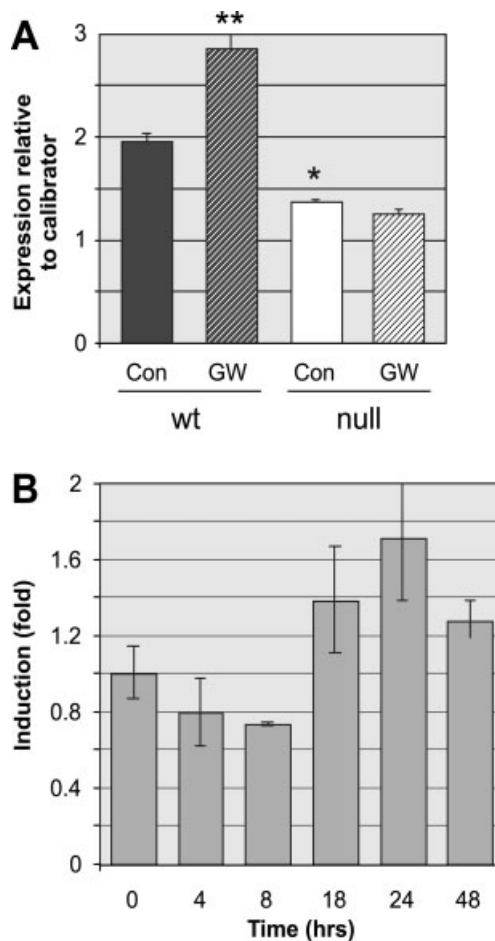


Figure 6. Induction of *Clic4* mRNA by the PPAR β agonist GW501516. (A) Aorta-derived wild-type and *Pparb* null ECs were treated with either DMSO solvent (Con) or with 1 μ M GW501516 (GW) for 24 h. RNA was extracted and analyzed by qPCR. *L27* was used as the normalizer, and pooled RNA from aortic EC cells served as the calibrator. Calibrator Ct values for *Clic4* and *L27* were 24.0 and 20.7, respectively. Data represent average values of triplicate samples, error bars show SD. *Significant difference between untreated wild-type and null cells; **significant difference between untreated and treated wild-type cells ($p < 0.05$; Student's *t*-test, two-tailed, equal variance). (B) HUVECs were treated with 1 μ M GW501516 for the indicated times and the expression of *Clic4* was determined by qPCR. Ct values for *Clic4* were in the range of 18–19. The graph shows relative expression values corrected for differences in *Gapdh* signals and normalized to 1 for non-stimulated cells (time 0). Data represent average values of triplicate samples, error bars show SD.

it formed semi-solid plugs that were invaded by ECs within 3 days. RNA was isolated from these plugs and analyzed by qPCR. In agreement with our observations made with cultured cells, *Clic4* levels were 51% higher in wild-type mice, while *Crbp1* expression was increased on average 2.6-fold in *Pparb* null mice (Fig. 7). These findings are in perfect agreement with our data obtained with cultured cells (Figs. 5 and 6).

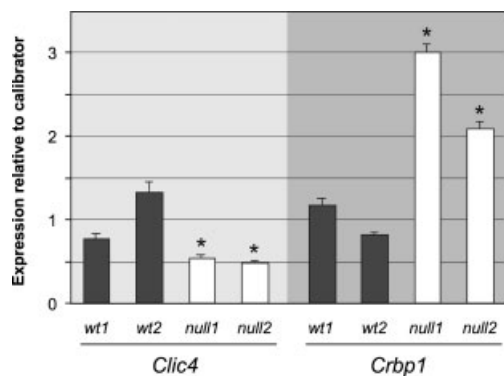


Figure 7. Regulation of *Clc4* and *Crbp1* mRNA by PPAR β *in vivo*. RNA was extracted from matrigel-infiltrating cells from wild-type and null mice 3 days after implantation and analyzed by qPCR. The data show an increased expression of *Clc4* in wild-type cells (black bars) compared to null cells (white bars), while the opposite picture was seen for *Crbp1*. Two independent matrigel plugs from each genotype were analyzed. *L27* and *Arp0* were used as normalizer, and pooled mouse fibroblast RNA served as the calibrator. Calibrator Ct values for *Clc4*, *CRBP1*, *L27* and *Arp0* were 24.5, 23, 20.5 and 17, respectively. Data represent average values of triplicate samples, error bars show SD. *Significant difference between *Pparb* wild-type and null mouse fibroblasts ($p < 0.05$; Student's *t*-test, two-tailed, equal variance).

4 Concluding remarks

In this communication we report for the first time the proteomic profile of *Pparb* null versus wild-type cells. Analysis of approximately 2000 spots separable on 2-D gels led to the identification of 31 proteins that reproducibly showed genotype-dependent expression. Twenty of these proteins were either putative regulators involved in intracellular signaling and tumorigenesis-associated biological processes (such as cell proliferation), or, as expected, metabolic enzymes. For several proteins of the first group a role in tumorigenesis has previously been suggested, even though in most cases the precise molecular functions with respect to oncogenesis remain to be investigated. These proteins include CLIC1, CLIC4, CRBP1, dimethylarginine dimethylaminohydrolase 2 (regulation of nitric oxide synthesis) [48], peroxiredoxin 1/proliferation associated gene 1 (tumor suppressor in mice) [49] and serine-threonine kinase receptor-associated protein (TGF- β signaling) [50]. Of these proteins, CLIC4 and CRBP1, deserve particular attention, since there is a relatively large body of evidence implicating these proteins in processes associated with tumorigenesis and/or showing aberrant expression in human tumors. In both cases, we also observed a clearly genotype-dependent regulation at the level of transcription in different experimental settings, including matrigel plugs used as an *in vivo* model of tumor angiogenesis.

CLIC4 expression promotes cell survival [22] and differentiation [34], and plays an essential role during tubular morphogenesis, presumably by constraining EC prolifera-

tion [33]. Likewise, PPAR β clearly has anti-proliferative and differentiation-promoting effects in different cell types [3–8], and disruption of the *Pparb* gene results in tumor endothelial hyperplasia and a defect in tumor vascularization (see Section 1). These correlations would be compatible with a model where the decreased expression of CLIC4 in *Pparb* null mice may contribute to the observed phenotype by interfering with an ordered proliferation and maturation of angiogenic ECs.

In contrast to CLIC4, the expression of CRBP1 is increased in *Pparb* null cells. CRBP1 is a negative regulator of the AKT signaling pathway, which in turn is activated by PPAR β through the direct transcriptional regulation of several key components, including *PDK1* and *PTEN* [51]. Therefore, the loss of PPAR β may lead to reduced AKT signaling by two independent mechanisms: (i) directly by reducing *PDK1* and *PTEN* transcription, and (ii) indirectly by CRBP1-mediated inhibition. Since the AKT signaling pathway plays a key role in angiogenesis [52], this may significantly contribute to the tumor vascularization defect in *Pparb* null mice.

In summary, our data are compelling evidence for a dysregulation of CLIC4 and CRBP1 expression in *Pparb* null mice in cell types and under conditions that are relevant to tumor angiogenesis. At present, our findings are of course correlative, but clearly provide a novel handle for dissecting the PPAR β signaling network in the context of tumorigenesis and tumor stroma function.

We are grateful to Dr. J. M. Peters (Pennsylvania State University) for providing Pparb null and wild-type mouse strains, and to Julia Dick and Stephanie Wick for excellent technical assistance. This work was supported by the Wilhelm-Sander-Stiftung, the Dr. Mildred Scheel Stiftung and the Deutsche Forschungsgemeinschaft (SFB-TR17).

5 References

- [1] Evans, R. M., Barish, G. D., Wang, Y. X., *Nat. Med.* 2004, 10, 355–361.
- [2] Barish, G. D., Narkar, V. A., Evans, R. M., *J. Clin. Invest.* 2006, 116, 590–597.
- [3] Tan, N. S., Michalik, L., Noy, N., Yasmin, R. *et al.*, *Genes Dev.* 2001, 15, 3263–3277.
- [4] Mao-Qiang, M., Fowler, A. J., Schmutz, M., Lau, P. *et al.*, *J. Invest. Dermatol.* 2004, 123, 305–312.
- [5] Schmutz, M., Haqq, C. M., Cairns, W. J., Holder, J. C. *et al.*, *J. Invest. Dermatol.* 2004, 122, 971–983.
- [6] Kim, D. J., Bility, M. T., Billin, A. N., Willson, T. M. *et al.*, *Cell Death Differ.* 2006, 13, 53–60.
- [7] Nadra, K., Anghel, S. I., Joye, E., Tan, N. S. *et al.*, *Mol. Cell Biol.* 2006, 26, 3266–3281.
- [8] Varnat, F., Heggeler, B. B., Grisel, P., Boucard, N. *et al.*, *Gastroenterology* 2006, 131, 538–553.

- [9] Michalik, L., Desvergne, B., Wahli, W., *Nat. Rev. Cancer* 2004, 4, 61–70.
- [10] Park, B. H., Vogelstein, B., Kinzler, K. W., *Proc. Natl. Acad. Sci. USA* 2001, 98, 2598–2603.
- [11] Gupta, R. A., Wang, D., Katkuri, S., Wang, H. *et al.*, *Nat. Med.* 2004, 10, 245–247.
- [12] Marin, H. E., Peraza, M. A., Billin, A. N., Willson, T. M. *et al.*, *Cancer Res.* 2006, 66, 4394–4401.
- [13] Harman, F. S., Nicol, C. J., Marin, H. E., Ward, J. M. *et al.*, *Nat. Med.* 2004, 10, 481–483.
- [14] Reed, K. R., Sansom, O. J., Hayes, A. J., Gescher, A. J. *et al.*, *Oncogene* 2004, 23, 8992–8996.
- [15] Barak, Y., Liao, D., He, W., Ong, E. S. *et al.*, *Proc. Natl. Acad. Sci. USA* 2002, 99, 303–308.
- [16] Liou, J. Y., Lee, S., Ghelani, D., Matijevic-Aleksic, N., Wu, K. K., *Arterioscler. Thromb. Vasc. Biol.* 2006, 26, 1481–1487.
- [17] Piqueras, L., Reynolds, A. R., Hodivala-Dilke, K. M., Alfranica, A. *et al.*, *Arterioscler. Thromb. Vasc. Biol.* 2007, 27, 63–69.
- [18] Peters, J. M., Lee, S. S., Li, W., Ward, J. M. *et al.*, *Mol. Cell. Biol.* 2000, 20, 5119–5128.
- [19] Suh, K. S., Yuspa, S. H., *Curr. Pharm. Des.* 2005, 11, 2753–2764.
- [20] Littler, D. R., Assaad, N. N., Harrop, S. J., Brown, L. J. *et al.*, *FEBS J.* 2005, 272, 4996–5007.
- [21] Fernandez-Salas, E., Suh, K. S., Speransky, V. V., Bowers, W. L. *et al.*, *Mol. Cell. Biol.* 2002, 22, 3610–3620.
- [22] Suh, K. S., Mutoh, M., Gerdes, M., Yuspa, S. H., *J. Invest. Dermatol. Symp. Proc.* 2005, 10, 105–109.
- [23] Suh, K. S., Mutoh, M., Gerdes, M., Crutchley, J. M. *et al.*, *Cancer Res.* 2005, 65, 562–571.
- [24] Shiio, Y., Suh, K. S., Lee, H., Yuspa, S. H. *et al.*, *J. Biol. Chem.* 2006, 281, 2750–2756.
- [25] Roberts, D., Williams, S. J., Cvetkovic, D., Weinstein, J. K. *et al.*, *DNA Cell Biol.* 2002, 21, 11–19.
- [26] Esteller, M., *Clin. Immunol.* 2003, 109, 80–88.
- [27] Cvetkovic, D., Williams, S. J., Hamilton, T. C., *Clin. Cancer Res.* 2003, 9, 1013–1020.
- [28] Jeronimo, C., Henrique, R., Oliveira, J., Lobo, F. *et al.*, *J. Clin. Pathol.* 2004, 57, 872–876.
- [29] Takahashi, T., Shivapurkar, N., Riquelme, E., Shigematsu, H. *et al.*, *Clin. Cancer Res.* 2004, 10, 6126–6133.
- [30] Liu, T., Bohlken, A., Kuljaca, S., Lee, M. *et al.*, *Br. J. Cancer* 2005, 93, 310–318.
- [31] Kwong, J., Lo, K. W., Chow, L. S., To, K. F. *et al.*, *Neoplasia* 2005, 7, 67–74.
- [32] Bistulfi, G., Pozzi, S., Ren, M., Rossetti, S., Sacchi, N., *Cancer Res.* 2006, 66, 10308–10314.
- [33] Bohman, S., Matsumoto, T., Suh, K., Dimberg, A. *et al.*, *J. Biol. Chem.* 2005, 280, 42397–42404.
- [34] Ronnov-Jessen, L., Villadsen, R., Edwards, J. C., Petersen, O. W., *Am. J. Pathol.* 2002, 161, 471–480.
- [35] Thornton, S. C., Mueller, S. N., Levine, E. M., *Science* 1983, 222, 623–625.
- [36] O'Farrell, P. H., *J. Biol. Chem.* 1975, 250, 4007–4021.
- [37] Klose, J., *Humangenetik* 1975, 26, 231–243.
- [38] Yan, J. X., Wait, R., Berkelman, T., Harry, R. A. *et al.*, *Electrophoresis* 2000, 21, 3666–3672.
- [39] Suh, K. S., Mutoh, M., Nagashima, K., Fernandez-Salas, E. *et al.*, *J. Biol. Chem.* 2004, 279, 4632–4641.
- [40] Molotkov, A., Ghyselinck, N. B., Chambon, P., Duester, G., *Biochem. J.* 2004, 383, 295–302.
- [41] Suzuki, M., Toyooka, S., Shivapurkar, N., Shigematsu, H. *et al.*, *Oncogene* 2005, 24, 1302–1308.
- [42] Farias, E. F., Marzan, C., Mira-y-Lopez, R., *Oncogene* 2005, 24, 1598–1606.
- [43] Hellemans, K., Rombouts, K., Quartier, E., Dittie, A. S. *et al.*, *J. Lipid Res.* 2003, 44, 280–295.
- [44] Shi, Y., Hon, M., Evans, R. M., *Proc. Natl. Acad. Sci. USA* 2002, 99, 2613–2618.
- [45] Tan, N. S., Michalik, L., Desvergne, B., Wahli, W., *J. Steroid Biochem. Mol. Biol.* 2005, 93, 99–105.
- [46] Degenhardt, T., Matilainen, M., Herzig, K. H., Dunlop, T. W., Carlberg, C., *J. Biol. Chem.* 2006, 281, 39607–39619.
- [47] Lee, C. H., Chawla, A., Urbiztondo, N., Liao, D. *et al.*, *Science* 2003, 302, 453–457.
- [48] Kostourou, V., Robinson, S. P., Cartwright, J. E., Whitley, G. S., *Br. J. Cancer* 2002, 87, 673–680.
- [49] Neumann, C. A., Krause, D. S., Carman, C. V., Das, S. *et al.*, *Nature* 2003, 424, 561–565.
- [50] Halder, S. K., Anumanthan, G., Maddula, R., Mann, J. *et al.*, *Cancer Res.* 2006, 66, 6156–6166.
- [51] Di-Poi, N., Tan, N. S., Michalik, L., Wahli, W., Desvergne, B., *Mol. Cell.* 2002, 10, 721–733.
- [52] Shiojima, I., Walsh, K., *Circ. Res.* 2002, 90, 1243–1250.